

Nonlinear Finite Element Analysis of High Strength Fiber Reinforced Concrete Corbels

Maha Mohammed Saeed Ridha

Received on:13/4/2005

Accepted on:11/12/2005

Abstract:

This research work presents a nonlinear finite element investigation on the behavior of high strength fiber reinforced concrete corbels. This investigation is carried out in order to get a better understanding of their behavior throughout the entire loading history.

The three- dimensional 20-node brick elements are used to model the concrete, while the reinforcing bars are modeled as axial members embedded within the concrete brick elements. The compressive behavior of concrete is simulated by an elastic-plastic work-hardening model followed by a perfectly plastic response, which terminate at the onset of crushing. In tension, a fixed smeared crack model has been used.

Key word: Corbels, Fiber , Finite Element ,Nonlinear

التحليل غير الخطي بطريقة العناصر المحددة للكتائف الخرسانية المسلحة عالية

المقاومة والمعززة بالالياف الفولاذية

الخلاصة :

تم في هذا البحث اختبار سلوك الكتائف الخرسانية المسلحة عالية المقاومة والمعززة بالالياف الفولاذية والمعرضة لاحمال القص باستخدام، انموذج التحليل غير الخطي بطريقة العناصر المحددة. هذا الانموذج استخدم للحصول على تفهم افضل لتصرف هذه الاعضاء من خلال تاريخ التحميل الكامل. تم استخدام العنصر الطابوقي ذو العشرين عقدة لتمثيل الخرسانة ، اما قضبان التسليح فقد مثلت كعناصر احادية البعد مضمورة في العنصر الخرساني ثلاثي الابعاد، تم تمثيل تصرف الخرسانة تحت تاثير اجهادات الضغط بالانموذج المرن-اللدن ذو التقوية الانفعالية حيث يتضمن هذا الانموذج افتراض سلوكاً مرناً للخرسانة في مستهل التحميل يعقبه سلوك مرن – لدن عند حدوث التشقق في الخرسانة ، ويستمر تحمل الاجهادات بمعدل انفعال متزايد لحين وصول مرحلة اللدونة التامة، وتنتهي هذه المرحلة بحدوث تهشم في الخرسانة. اما سلوك الخرسانة تحت تاثير اجهادات الشد فقد تم تبني انموذج التشقق المنتشر لتمثيله.

Nomenclature

d_f	Diameter of fiber
f'_c	Uniaxial compressive strength of plain concrete.
f'_{cf}	Uniaxial compressive strength of fiber reinforced concrete
f_{tf}	Uniaxial tensile strength of Steel fiber concrete
L_f	Fiber length
N_f	Number of fiber per unit cross-sectional area
a_1, a_2	Tension-stiffening parameter
b	Aterial constant
β_1	hear retention factor
g_1, g_2, g_3	Shear retention parameters
λ	Compressive strength reduction factor of concrete
σ_n	Stress normal to cracked plane.
ϵ_n	Strain normal to cracked plane
ϵ_{cr}	Cracking strain
σ_{cr}	Cracking stress.
ϵ_{tf1}	Tensile strain at peak tensile stress.

Introduction:

In recent years, the use of high strength concrete has increased rapidly as a result of the demand for higher strength, relatively lighter weight, and durable concrete. The major difference between the normal strength concrete and high strength concrete is that the high strength concrete tends to behave as an elastic and more brittle material compared with normal strength concrete⁽¹⁾. The observed inverse relationship between strength and ductility is a serious drawback if the use of high strength concrete is to be considered in some structural applications. However, such a drawback can be overcome by addition of strong discontinuous fibers. It can be safely said today that one of the most desirable benefits of adding fibers to concrete is to increase its energy absorbing capability, ductility and toughness as often characterized by the shape of the area under the post-peak portion of its stress-strain curve⁽²⁾. Corbels (or brackets) which are built monolithically with columns (or walls), are usually used to support precast beams, slabs and any other form of precast structural system. In the last three decades several studies were made to investigate the behavior of reinforced concrete corbels⁽³⁾. The choice of the panels or membrane elements was intended to isolate the effect of other unpreferred combination of stresses, and focus on the reduction of concrete

compressive strength in the presence of transverse tensile straining of reinforcement on what is called softening phenomenon.

Finite Element Model:

In the present research work, a full three-dimensional finite element idealization has been used. This idealization gives accurate simulation for geometry, type of failure and location of reinforcing bars. The 20-node quadratic brick element shown in Fig. (1) is adopted to represent concrete in the present study.

The reinforcement representation that is used in this study is the embedded representation, Fig. (1). The reinforcing bar is considered to be an axial member built into the concrete element. The reinforcing bars were assumed to be capable of transmitting axial force only.

The numerical integration is generally carried out using the 27(3x3x3) point Gaussian type integration rule.

The nonlinear equations of equilibrium have been solved using an incremental-iterative technique operating under load control. The nonlinear solution algorithm that is used in this research work is the modified Newton-Raphson method in which the stiffness matrix is updated at the 2nd, 12th, 22nd, ...etc. iterations of each increment of loading.

Material Model Adopted in the Analysis**Behavior in Compression:**

In compression, the behavior of concrete is simulated by an

elastic-plastic work hardening model followed by a perfectly plastic response, which is terminated at the onset of crushing. The growth of subsequent loading surfaces is described by an isotropic hardening rule. A parabolic equivalent uniaxial stress-strain curve has been used to represent the work hardening stage of behavior and the plastic straining is controlled by an associated flow rule.

The concrete strength under multidimensional state of stress is a function of the state of stress and cannot be predicted by simple tensile, compressive and shearing stress independent of each other. So the state of stress must be scaled by an appropriate yield criterion to convert it to equivalent stress that could be obtained from simple experimental test. The yield criterion that has been used successfully by many investigators ^{(4),(5)} can be expressed as $f(\{\sigma\}) = (\alpha I_1 + 3\beta J_2)^{0.5} = \sigma_0$... (1)

where α and β are material parameters which are dependent on the type of concrete, mainly on the volume fraction of fiber V_f , and their values are shown in Table (1) ^{(6),(7)}. I_1 is the first stress invariant and J_2 is the second deviatoric stress invariant. σ_0 is an equivalent effective stress at the onset of plastic deformation which can be determined from a uniaxial compression test.

In a reinforced concrete member, a significant degradation in compressive strength can result due to the presence of transverse tensile straining after cracking. In the present study, Vecchio et. al. models are used for HSC ⁽⁶⁾ members, which illustrates the use of the reduction factor, λ . The compressive reduction factor, λ , for HSC is given as:

$$\lambda = \frac{1}{1 + K_c \cdot K_f} \dots (2)$$

where K_c is a factor representing the effect of the transverse cracking and straining and K_f is a factor representing the effect of concrete compressive strength f'_c .

$$K_c = 0.35 (\epsilon_1 / \epsilon_3 - 0.28)^{0.8} \dots (3)$$

and

$$K_f = 0.1825 \sqrt{f'_c} \geq 1.0 \dots (4)$$

where ϵ_1 is the tensile strain in the direction normal to the crack and ϵ_3 is the compressive strain in the direction parallel to the crack.

Behavior in Tension:

In tension, linear elastic behavior prior to cracking is assumed. Cracking is governed by the attainment of a maximum

$$f'_{cf} = (f'_c)^{0.941} \cdot (V_f \cdot L_f / d_f)^{0.054} \dots (8)$$

principal stress criterion. A smeared crack model with fixed orthogonal cracks is assumed to represent the cracked sampling point. The post-cracking tensile

stress-strain relations, Fig. (2),^{(9),(10)} and the reduction in shear modulus with increasing tensile strain Fig. (3),⁽¹¹⁾ have been adopted in the present work. The tensile strain at peak tensile stress (ϵ_{tf1}) is given by:

$$e_{tf1} = e_t (1 + 0.35 N_f . d_f . L_f) \dots\dots (5)$$

where

N_f : is the number of fiber per unit area ; given by :

$$N_f = h_0 \left[\frac{4V_f}{pd'_f} \right] \dots\dots (6) .$$

Behavior of Steel Fiber Reinforced Concrete:

In compression, an empirical equation for peak strain value in uniaxial compression of high strength fiber reinforced concrete (ϵ_{pf}) suggested by AL- AZZAWI⁽¹²⁾ is adopted in the present study as:

In his study, an empirical

$$\epsilon_{pf} = 0.00212 + 0.001 V_f * L_f / d_f ..(7)$$

equations for (f'_{cf}) suggested by Bunni⁽¹³⁾ is adopted and is given by :

According to test results reported in reference⁽¹⁴⁾ the concrete peak value of the tensile stress of high strength fiber reinforced concrete (f'_{tf}) is proposed in terms of compressive strength of reinforce (f'_c) and fiber volume fraction (V_f in percent) as follows:

$$f_{tf} = 0.58 \sqrt{f'_c} + 302 . V_f \dots\dots(9)$$

Numerical Example

Description of Test Specimens:

A total of 36 reinforced concrete corbels were tested by Muhammad⁽³⁾ under monotonic loading up to failure. In order to check the validity of the present material model, four of these corbels were chosen for this research work to carry out the finite element analysis. These corbels were C-5, C-6, C-7, and C-8. All tested corbels had a longitudinal steel ratio of 1.01% and shear –span/depth (a/d) ratio of 0.5. All corbels failed in shear mode. Fig.(4) shows the loading arrangement and reinforcement details.

The same type of fibers was used throughout the test program. The fibers were hooked, 60mm in length and 0.8mm in diameter making an aspect ratio (L_f/d_f) of 75, . The steel fibers had an ultimate tensile strength of 1050MPa.

Finite Element Idealization and Material Properties:

By making use of the symmetry of loading, geometry and reinforcement distribution of the tested corbels, only one half of the length will be considered in the numerical analyses. In the present study, the chosen segments were modeled using 8 brick elements. The finite element mesh, boundary conditions, and loading arrangement are shown in Fig.(5). The dimensions, material properties and the additional material and numerical parameters are listed in Table (2).

The longitudinal bars were simulated as embedded elements into the brick elements. The external loads were applied in equal increments of 5 % of the expected failure load. These increments were reduced at stages close to the ultimate loads.

The numerical analyses have been generally carried out using the 27-point integration rule and a convergence tolerance of 2 %.

Results of Analysis:

The experimental and numerical load –deflection curves for corbels C-5 to C-8 are shown in Fig.(6).

These figures show good agreement for the finite element solution compared with the experimental results throughout the entire range of behavior. They reveal that both the initial and post-cracking stiffnesses are reasonably predicted. The computed failure loads for all corbels are close to the corresponding experimental collapse load as listed in Table (3).

Parametric Studies

To investigate the effects of some of the material and solution parameters on the nonlinear finite element analysis of high strength fiber concrete corbels, corbel C-7 have been chosen to carry out a parametric study. This study helps to clarify the effect of various parameters that have been considered on the behavior and ultimate load capacity of the analyzed corbels.

Influence of Fiber Content

The presence of fibers enhances the ductility and energy absorption capacity of reinforced concrete members and act as crack arresters. Therefore, the addition of a small amount of fibers can increase the flexural, shear and torsional capacity of the members.

To study the effect of using different amounts of fibers, six tests have been carried out with volume fraction of fiber ranging from 0.0 to 1.5%. Fig. (7) shows that the post cracking stiffness and the predicted cracking and ultimate load are considerably increased as the fiber content is increased. The finite element results revealed that an increase up to 57% in ultimate load capacity can be achieved by using a fiber content of 1.5% for corbel C-7.

Effect of Grade of Concrete

In the present research work, a study was made to investigate the use of concrete of higher compressive strength. This was achieved by numerically testing an assumed corbel with a wide range of concrete compressive strength. This corbel is similar in dimensions, arrangement of reinforcement and other details to C-7. The tension stiffening parameters α_1 and α_2 were set equal to 110 and 0.9 respectively. While the shear retention parameters γ_1 , γ_2 and γ_3 were set equal to 100, 0.9 and 0.15 respectively.

The results of this investigation are shown in Fig. (8). Four grades

of concrete were considered in this study. These are 30, 50, 70 and 90 MPa. The analysis revealed that the failure was due to concrete crushing for all grades of concrete. Therefore the cracking load and post-cracking stiffness are increased by increasing concrete compressive strength. The finite element results revealed that an increase up to 60% in ultimate load capacity can be achieved by using compressive strength equal to 90 MPa, compared to a compressive strength of 30 MPa.

Influence of Longitudinal Reinforcement

The influence of using different longitudinal reinforcement ratios on the load-deflection curve is investigated. An assumed corbel reinforced with various longitudinal reinforcement ratios was numerically tested. The results are shown in Fig. (9). The longitudinal reinforcement ratio varied from 0.68 to 2.7%. The concrete compressive strength and reinforcement yield stress were 70 and 419 MPa respectively. By studying the predicted response of the corbel, it can be seen that the increase in the longitudinal reinforcement ratio leads to a stiffer post-cracking response and significant increase in the ultimate load capacity of the corbel. The finite element results revealed that an increase up to 50% in ultimate load capacity can be achieved by using longitudinal reinforcement ratio equal to

2.7%, compared to a ratio of 0.68%.

Influence of shear span-depth ratio a/d

In order to investigate the influence of using different shear span-depth (a/d) ratio on the behavior of load-deflection curve of the corbel, an assumed corbel reinforced with various shear span-depth (a/d) ratios were numerically tested. The results are shown in Fig. (10). The shear span-depth (a/d) ratio varied from 0.3 to 0.75.

By studying the predicted response of the corbel, it can be seen that the increase in the shear span-depth (a/d) ratio leads to a decrease in the post-cracking stiffness response and significant decrease in the cracking load and ultimate load capacity of the corbel. The finite element results revealed that an increase up to 78.9% in ultimate load capacity can be achieved by using shear span-depth (a/d) ratio

Conclusions

1. The three dimensional nonlinear finite element model used in the present work is capable of simulating the behavior of fiber reinforced concrete corbels subjected to monotonic loading. The finite element analysis carried out showed good agreement with the experimental results throughout the entire range of behavior.
2. The increase in concrete compressive strength results in a significant increase in the ultimate load capacity of the corbels when

the failure is due to concrete crushing.

3. The addition of a small amount of steel fibers to concrete significantly increases the cracking load. This may be attributed to crack arresting mechanism of fibers. An increase of 125 % in cracking load can be achieved by using fiber content of 1.5% for corbel C-7.

4. The addition of steel fibers to concrete increases the collapse load. The value of the collapse load depends on the properties of fibers and type of failure. An increase of 57% in ultimate load capacity was obtained when a fiber content of 1.5% was added to corbel C-7.

5. The increase in longitudinal reinforcement ratio was found to increase ultimate load capacity and post-cracking stiffness. An increase up to 50% in ultimate load capacity can be achieved by using longitudinal reinforcement ratio of 2.7%.

6. The increase in shear span – depth (a/d) ratio was found to decrease ultimate load capacity and post-cracking stiffness. A decrease up to 78.9% in ultimate load capacity can be achieved by using shear span – depth (a/d) ratio of 7.5%.

References

1. Rasmussen, L. J., and Baker, G., "Torsion in Reinforced Normal and High-Strength Concrete-Part I Experimental Test Series", ACI Structural

Journal, Jan-Feb. 1995, pp. 56-61.

2. Naaman, A. E., and Homrich, J. R., "Properties of High-Strength Fiber Reinforced Concrete" ACI Publication, SP 87-13, 1985, pp. 234-235.

3. Muhammad, A. H., "Behavior of Strength of High-Strength Fiber Reinforced Concrete Corbels Subjected to Monotonic or Cyclic (Repeated) Loading", Ph.D. Thesis, University of Technology, 1998.

4. Thannon, A. Y., "Ultimate Load Analysis of Reinforced Concrete Stiffened Shells and Folded Slabs Used in Architectural Structures", Ph.D. Thesis, University of Wales, Swansea, 1988.

5. Hinton, E. and Owen, D.R.J., "Finite Element Software for Plates and Shells" Pineridge Press, Swansea, 1984.

6. Allose, L. E., "Three Dimensional Nonlinear Finite Element Analysis of Steel Fiber Reinforced Concrete Beams in Torsion", M.Sc. Thesis, University of Technology, 1996.

7. Abdul-Wahab H.M.S., "Strength of reinforced concrete corbels with fibers", ACI Structure J., Vol. 86, No. 1, Jan.-Feb. 1989, pp. 60-66.

8. T. Vecchio, F. J., Collins, M. P., and Aspioties, "High Strength Concrete Elements Subjected to Shear", ACI Structural Journal, July-Aug. 1994, pp. 423-433.

9. Al-Shaarbaf, I. A.S., "Three Dimensional Nonlinear Finite Element Analysis of Reinforced Concrete Beams in Torsion",

- Ph.D. Thesis, University of Bradford, 1990.
10. Al-Moussely, B. S., "Three Dimensional Nonlinear Finite Element Analysis for Steel Fiber Reinforced Concrete Beams Subjected to Combined Bending and Torsion", M.Sc. Thesis, University of Technology, 1998.
11. Naji, J. H., and I. May, "The Effect of Some Numerical and Material Parameters on the Nonlinear Finite Element Analysis of Reinforced Concrete Beams", Proceedings of the Third Arab Engineering Conference, Vol. 1, March 1998, No. 5, pp. 10-17.
12. Al-Azzawi, Z. M. K., "Capacity of High Strength Fiber Reinforced Beam Column Joints", M. Sc. Thesis, University of Technology, 1997.
13. Bunni, Z. J., "Shear Strength in High-Strength Fiber Reinforced Concrete Beams", M. Sc. Thesis, University of Technology, Baghdad, 1998, 105 PP.
14. Wafa, F. F., and Ashour, S. A. "Mechanical Properties of High Strength Fiber Reinforced Concrete", ACI Materials Journal, Vol. 89, 1992, No. 5, pp. 455-499.
15. Carrasquillo, R. L., Nilson, A. H., and Slate, F.O., "Properties of High Strength Concrete Subject to Short-Term Loads", ACI Journal, Vol. 78, No. 3, May-June 1981, pp. 171-178.

Table (1) Material Parameters.

V_f	α	β
0.0	0.3546798 σ_o	1.3546798
0.5	1.0993042 σ_o	2.0993042
1.0	1.4960526 σ_o	2.4900526
1.5	1.7960526 σ_o	2.7960526

Table (2). Dimensions, material properties and the additional material and numerical parameters used in Muhammad's corbels.

		C-5	C-6	C-7	C-8
Concrete					
Shear Span a (mm)		115	115	115	115
Width b (mm)		150	150	150	150
Effective Depth d (mm)		230	230	230	230
Young's Modulus ⁽¹⁵⁾ , E_c *(MPa)		34116	34934	35440	35729
Compressive Strength, f'_c (MPa)		66.2	69	71.4	74.1
Tensile Strength, f_t (MPa)		4.755	6.407	8.006	9.566
Poisson's Ratio, n		0.2	0.2	0.2	0.2
Uniaxial Crushing Strain, ϵ_{cu}		0.003	0.00337	0.00375	0.004
Main Reinforcement					
Bar Diameter (mm)		12.7	12.7	12.7	12.7
Young's Modulus, E_s (MPa)	200000	200000	200000	200000	
Steel Ratio, Γ_W (%)		1.01	1.01	1.01	1.01
Yield Stress, f_y (MPa)		419	419	419	419
Hardening Parameter H'		0.0	0.0	0.0	0.0
Steel Fiber					
Volumes Fraction of Fibers, V_f %		0.0	0.5	1.0	1.5
Aspect Ratio, L_f / d_f			75	75	75
Tension-Stiffening Parameters					
Model		TS	TS1	TS1	TS1
α_1		70	80	110	120
α_2		0.7	0.75	0.9	0.95
Shear-Retention Parameters					
γ_1		60	90	100	105
γ_2		0.8	0.85	0.9	0.95
γ_3		0.1	0.1	0.15	0.15

* $E_c = 3320\sqrt{f'_c} + 6900$ for $21 \text{ MPa} < f'_c < 81 \text{ MPa}$ (10)

Table (3). Comparison between experimental and predicted collapse loads.

Corbels	Experimental Collapse Load $P_{u, exp}^{(3)}$ (kN)	Numerical Collapse Load (kN)	
		$P_{u, num}$	$P_{u, num.}$ <hr/> $P_{u, exp.}$
C-5	273.1	274	1.003
C-6	333.7	333	0.998
C-7	441	445	1.009
C-8	465.5	469	1.008

Table (3). Comparison between cracking and ultimate loads
For different amounts of fibers.

V_f %	Numerical Cracking Load (kN)	Numerical Ultimate Load (kN)
0.0	80	318
0.5	100	392
1.0	140	445
1.5	180	499

Table (3). Comparison between cracking and ultimate loads
for different shear span-depth (a/d) ratios.

a/d	Numerical Cracking Load (kN)	Numerical Ultimate Load (kN)
0.3	220	601
0.5	140	445
0.75	100	336

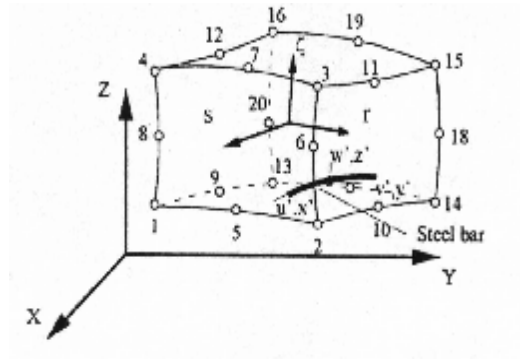
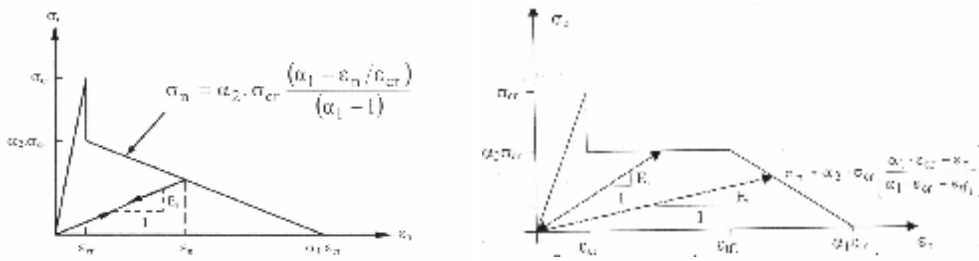


Fig. (1) The twenty-node brick element.



a) Plain concrete

b) Fiber reinforced concrete.

Fig. (2) Post-cracking models for cracked concrete.

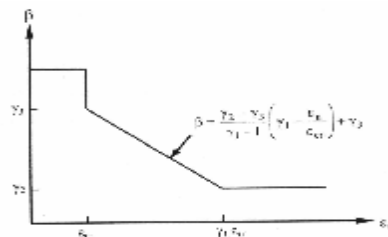


Fig. (3) Shear retention model for cracked concrete.

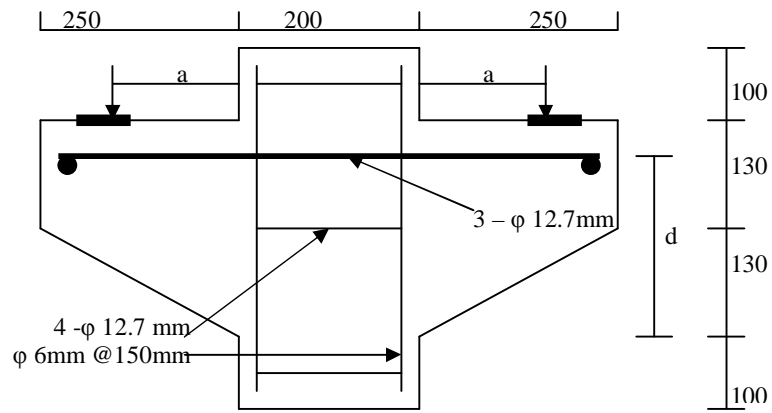


Fig.(4).Dimensions and reinforcement details of Muhammad's corbels (3)
{All dimensions in (mm)}

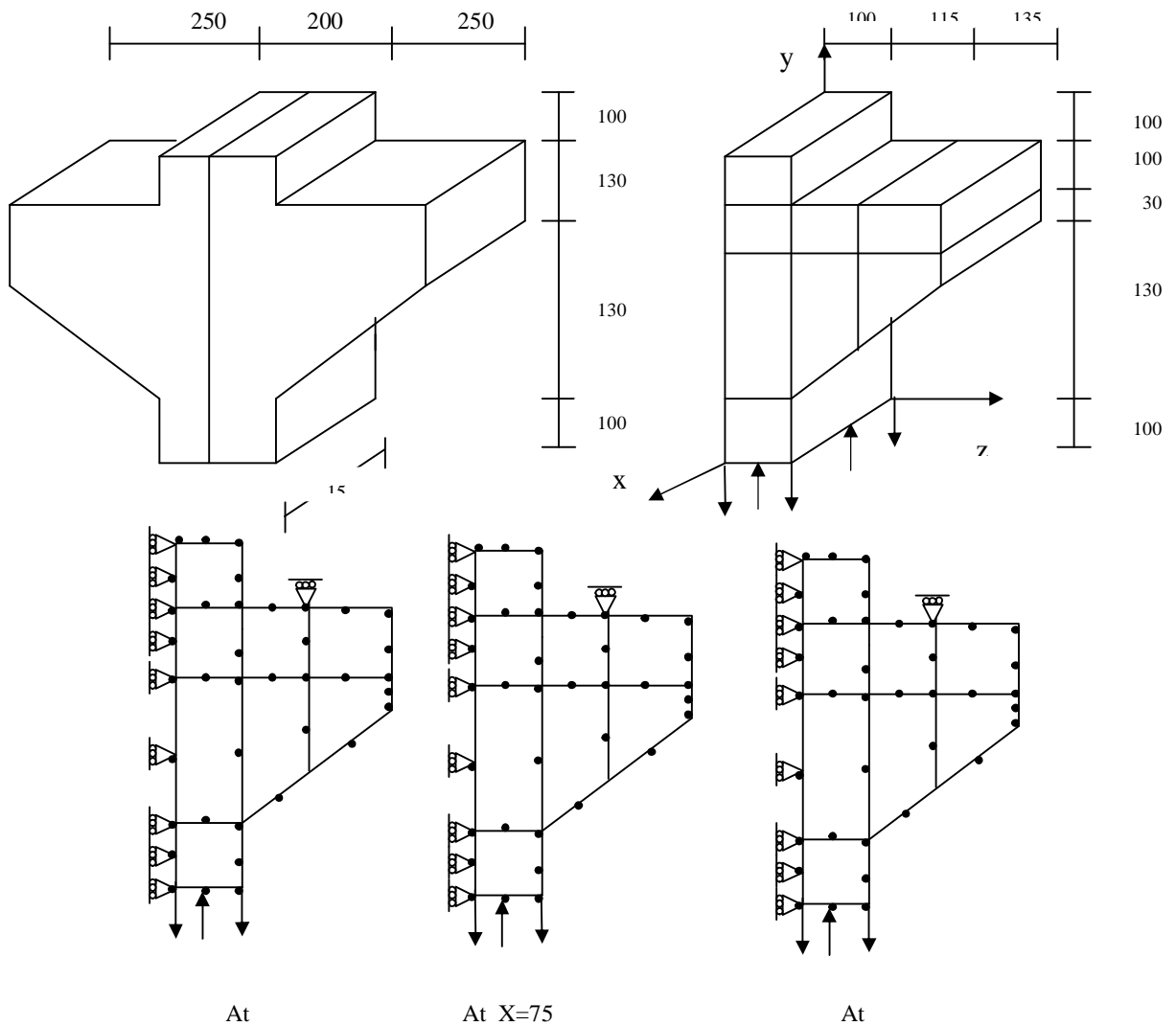


Fig.(5). Finite element mesh and conditions in Muhammad's corbels.
{All dimensions in (mm)}

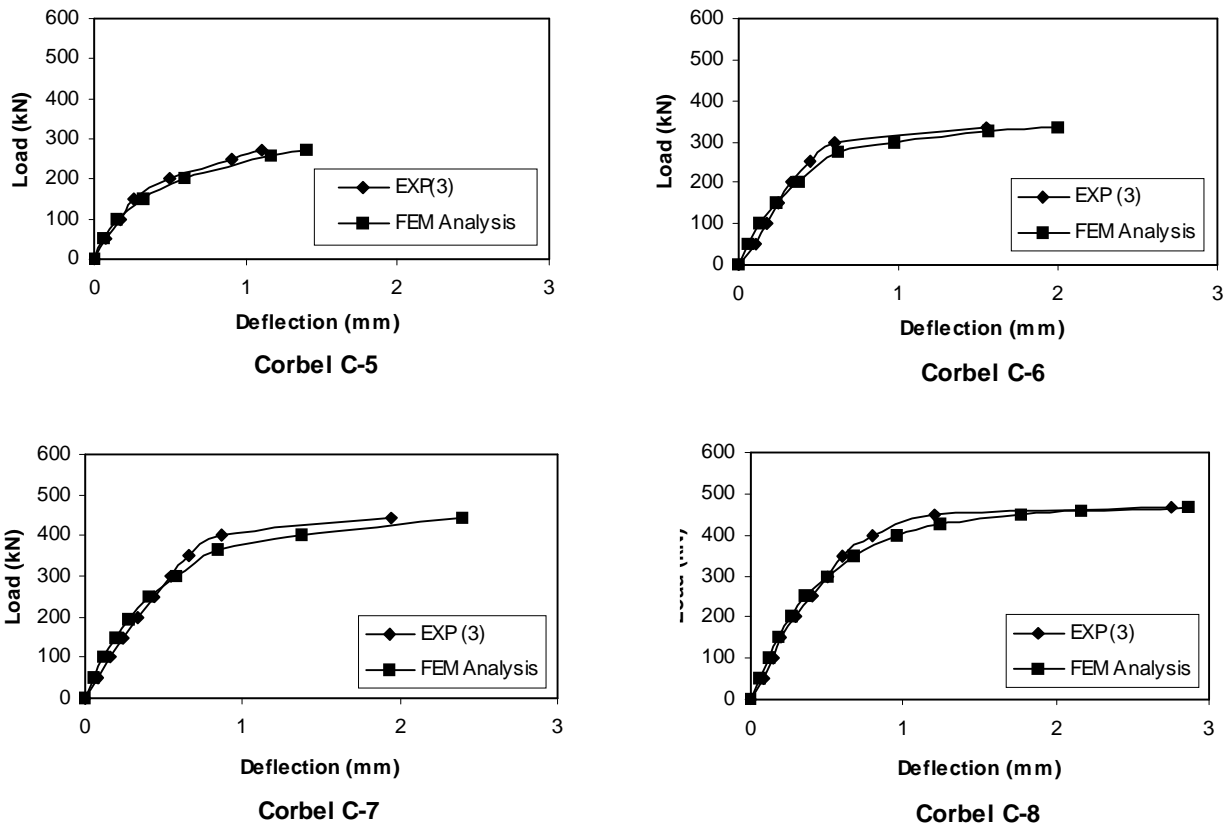


Fig.(6).Muhammads corbels, analytical and experimental load- deflection curves.

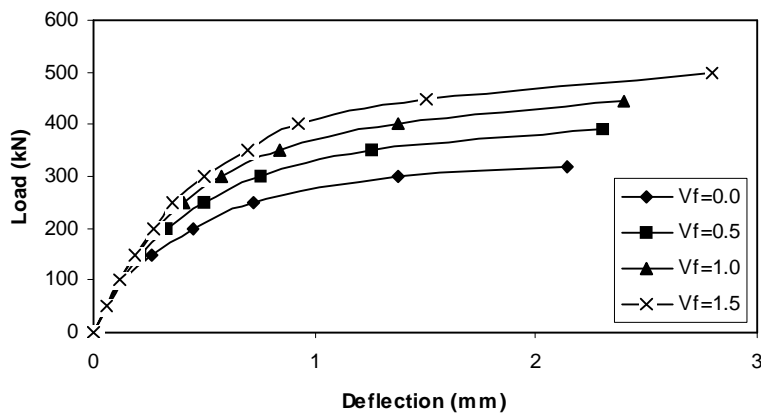


Fig.(7) Influence of fiber content on load-deflection curve for Corbel C-7

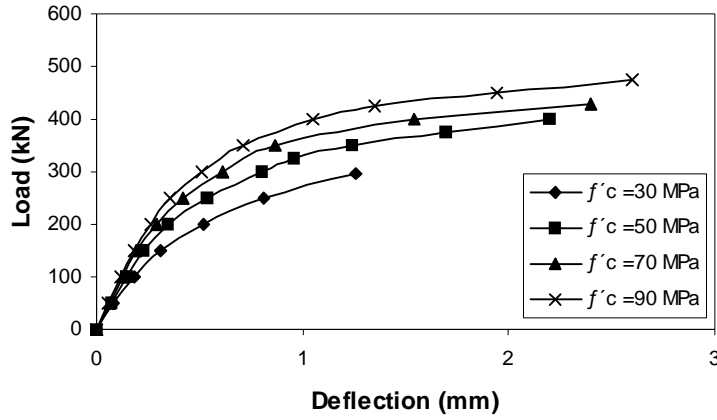


Fig.(8) Effect of increasing the grades of concrete on the load - deflection behavior for corbel C-7

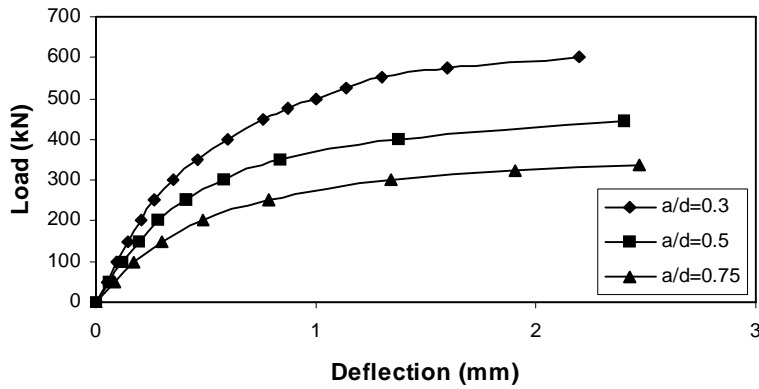


Fig. (10) Influence of shear span-depth (a/d) ratio on load-deflection curve for corbel C-7